Monatsh Chem (2011) 142:885–893
DOI 10.1007/s00706-011-0545-z

ORIGINAL PAPER

Modes of complexation of rutin with the flavonoid reagent diphenylborinic acid 2-aminoethyl ester

Paolo Matteini · Giovanni Agati · Patrizia Pinelli · Andrea Goti

Received: 21 April 2011 / Accepted: 30 May 2011 / Published online: 28 June 2011

Abstract The interaction of the model flavonoid glycoside rutin with the flavonoid reagent diphenylborinic acid 2-aminoethyl ester (DPBA) was investigated using a combination of HPLC–DAD–ESI–MS analysis, UV–visible spectroscopy, and semiempirical calculations. Mass spectra and spectroscopic data made it possible to describe the complexation pathway as addition of diphenylboron groups to the two available 3′,4′-*o*-diphenolic and the 5-hydroxy-4-keto coordinating sites of rutin. Semiempirical calculations were carried out to obtain the conformation of the most stable DPBA/rutin adducts. The results showed that a number of complexation dynamics can occur as a function of the characteristics of the medium (type and pH of the solvent) and of the amount of DPBA. This work suggests the possibility of substantially improving existing procedures for recognition of flavonoid compounds by choice of suitable experimental conditions.

Keywords Natural products · Structure elucidation · Semiempirical calculations · Naturstoff reagent

P. Matteini (✉) · G. Agati
Institute of Applied Physics, National Research Council, via Madonna del Piano 10, 50019 Sesto Fiorentino, Italy
e-mail: p.matteini@ifac.cnr.it

P. Pinelli
Department of Pharmaceutical Sciences, University of Florence, via Ugo Schiff 6, 50019 Sesto Fiorentino, Italy

A. Goti
Department of Chemistry "Ugo Schiff", University of Florence, via della Lastruccia 3, 50019 Sesto Fiorentino, Italy

Introduction

Flavonoids have been shown to play a major role in the interaction of plants with stress-inducing agents, both biotic (e.g., pathogens and predators) and abiotic (e.g., nutrient deficiency, presence of heavy metals, high solar irradiance) [1–4]. The widespread distribution of flavonoids on the leaf surface and in the epidermal cells may primarily constitute an effective shield against the penetration of harmful solar radiation [5, 6]. These compounds usually absorb in the 250–360 nm region, and thus are capable of acting as UV filters, thereby protecting the underlying photosynthetic tissues from damage. More recently, it has been hypothesized that flavonoids have antioxidant activity in species exposed to a wide range of environmental stresses [4, 7–10]. This hypothesis is primarily supported by the capacity of flavonoids to effectively scavenge free radicals both in solution and in trials, as a result of their ability to quench unpaired electrons and/or to inhibit the generation of free radicals (e.g., through their metal ion-chelating properties) [3, 11, 12]. In particular, *ortho*-dihydroxylated flavonoids (for example luteolin, quercetin, and rutin) have proven to be efficient antioxidants because of their catechol moiety, which confers enhanced hydrogen-donor capacity and improved metal-chelating potential [3, 11].

Over the past two decades, many experiments have focussed on the characterization of flavonoids of plants with the objective of understanding their roles in the mechanism of acclimation to different stresses [8, 13, 14]. The most popular method of investigation consists in measurement of the fluorescence of flavonoids induced by staining specimens with diphenylborinic acid 2-aminoethyl ester (DPBA, also called Naturstoff reagent or Neu's

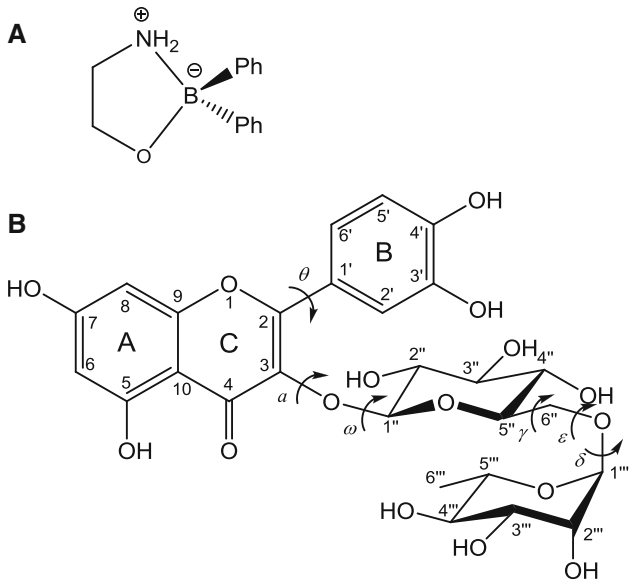

Fig. 1 Representation of diphenylborinic acid 2-aminoethyl ester (**a**) and rutin (**b**)

reagent, Fig. 1a) (natural flavonoids have no or low autofluorescence) [8, 13, 15]. DPBA has a long history of successful applications as a spray reagent for flavonoid compounds in paper and thin-layer chromatography [16, 17] before being effectively applied in histochemistry for location of flavonoid compounds in tissue. Its introduction dates back to 1957, when Neu proposed the use of complexes of diarylborinic and oxyalkylamines as specific reagents for the detection of phenylbenzo-γ-pyrone derivatives [18]. After DPBA staining of plant tissue, excitation with UV or blue light induces a fluorescence signal which has been extensively ascribed to complexes of flavonoid compounds [13, 19]. Blue excitation combined with the detection of the green-to-yellow–orange fluorescence has recently become the gold standard for detecting flavonoids with minimum interference from other compounds [13, 15, 20–22].

Despite the routine use of DPBA for the detection of flavonoids, understanding of its interaction with the different reactive sites of the flavonoid molecule remains an unresolved problem. To the best of our knowledge, no clear experimental proof of the actual interaction of a flavonoid with DPBA has yet been collected, even though formation of specific complexes has been speculated on some occasions [17]. In the work discussed in this paper we investigated the complexation between DPBA and rutin, used as a representative flavonoid. Rutin (quercetin 3-rhamnoglucoside, Fig. 1b) is an *ortho*-dihydroxylated flavonoid with strong antioxidant properties and other beneficial activity in human beings [6, 11, 23–25]. The disaccharide rutinose linked to the O3 position confers solubility in aqueous environments, which explains its widespread occurrence in the cytosolic and vacuolar compartments of vegetable and fruit cells [11, 20]. The presence in rutin of two competing chelating sites, i.e. the 3′,4′-*o*-diphenolic and the 5-hydroxy-4-keto groups (hereafter also referred to as catechol and ketoenol) makes it possible to compare the complexation power of different coordinating moieties. Rutin was also chosen because of substantial knowledge of the structural behaviour of its free form, which was investigated in a recent study [26]. By a combination of experimental (MS analysis and UV–visible spectroscopy) and theoretical (semiempirical calculations) methods, large variability in the dynamics of the DPBA–rutin interaction was found to be a function of conditions including DPBA concentration, pH, and the type of solvent.

Results and discussion

Mass spectral characterization

Negative-ion mass spectra of a DPBA–rutin mixture at 1:1 molar ratio afforded the quasi-molecular $[M - H]^-$ ion as the main contribution and an $[M + 164]^-$ ion which can be

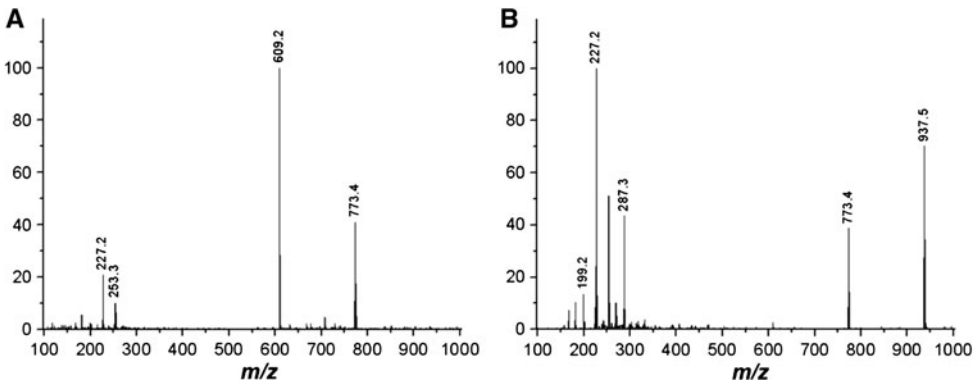

Fig. 2 Negative-ion mass spectra of a mixture of rutin and DPBA at 1:1 (**a**) and 100:1 (**b**) [DPBA]/[rutin] molar ratios in aqueous solution. The quasi molecular ion $[M - H]^-$ of rutin appears at $m/z = 609.2$. Fragments at $m/z = 773.4$ and 937.5 are ascribed to the addition of one and two diphenylboron residues to the free rutin molecule

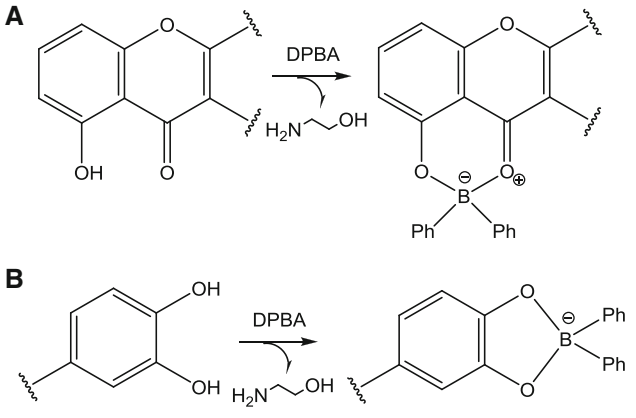

Fig. 3 Complexation pathways between the 5-hydroxy-4-keto (**a**) and 3′,4′-*o*-diphenolic (**b**) reactive sites of rutin and DPBA, as deduced from HPLC–DAD–ESI–MS analysis

ascribed to the formation of a mono adduct with DPBA (Fig. 2a). A new $[M + 164 + 164]^-$ ion peak was further observed when a 100-fold excess of DPBA was used; this was interpreted as the presence of a bis adduct (Fig. 2b). These results suggest that up to two different molecular sites of rutin can effectively coordinate DPBA as a function of its concentration. These sites can be assigned to the 3′,4′-*o*-diphenolic group and the 5-hydroxy-4-keto group, which can potentially coordinate DPBA according with the well-known chelating properties of flavonols and flavones with boron and metal compounds [27–31]. The *m*/*z* 164 fragment added to the molecular ion suggests a complexation pathway that involves the addition of a diphenylboron fragment to the catechol and/or to the ketoenol reactive sites after the loss of an ethanolamine chain, as can be seen in Fig. 3.

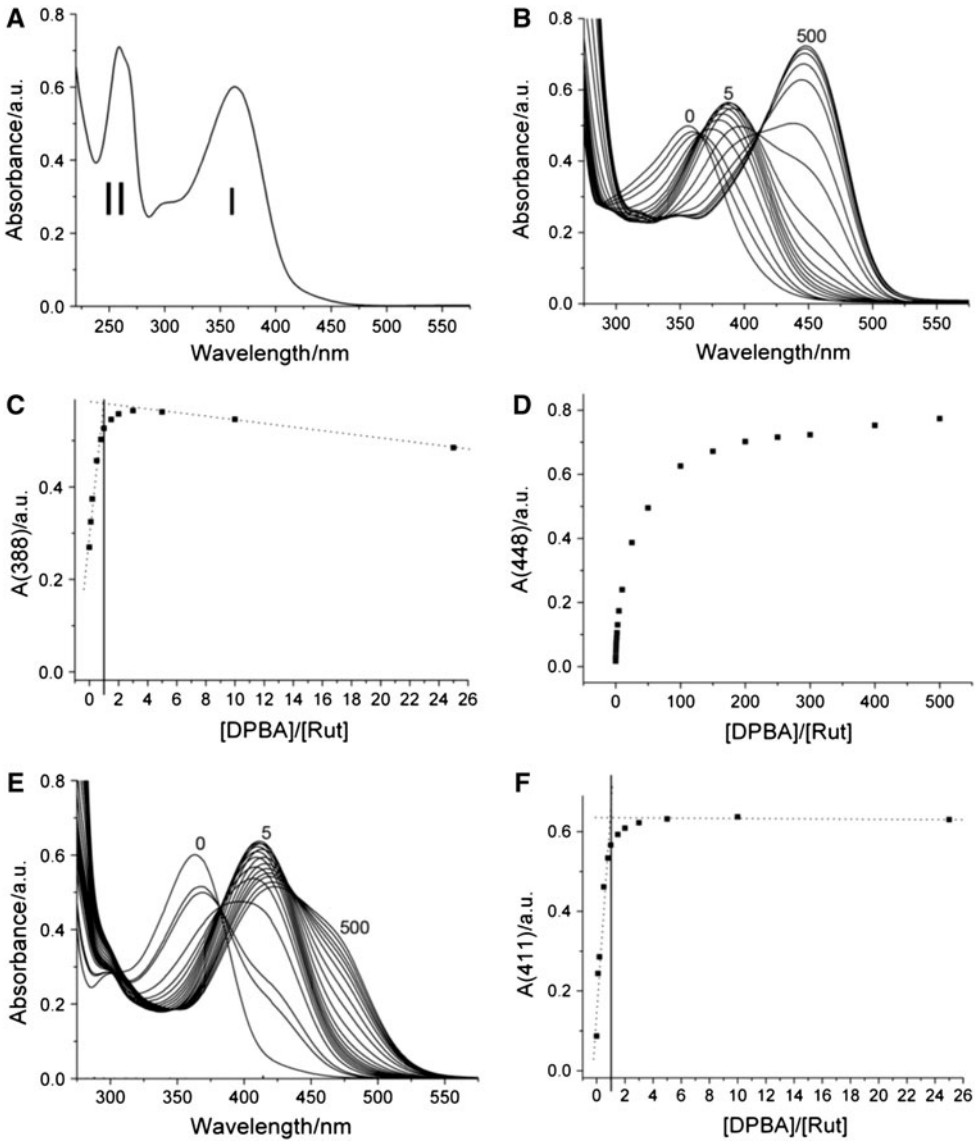

Fig. 4 Representative UV–visible spectrum of rutin in ethanol (**a**). Spectroscopic titration of rutin in phosphate buffer (pH 7, **b**) and ethanol (**e**) by increasing the DPBA concentration. The DPBA-to-rutin molar ratios are indicated above the relevant spectrum profiles. Plots of absorbance at 388 nm (**c**) and 448 nm (**d**) in phosphate buffer, and at 411 nm (**f**) in ethanol versus the molar ratio

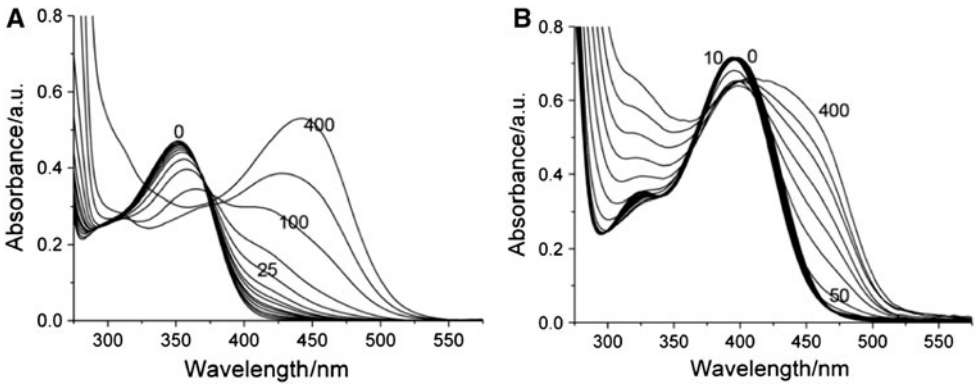

Fig. 5 Representative UV–visible spectrum of rutin in acetate buffer (pH 4, **a**) and sodium acetate (pH 9, **b**) with increasing DPBA concentration. The DPBA-to-rutin molar ratios are indicated above the relevant spectrum profiles

UV–visible characterization

In Fig. 4a a representative absorbance profile of free rutin is shown. In general, as a member of the flavonoid family, rutin gives two major absorption bands in the UV region: band I at ~355 nm, which is associated with absorption of light by the B ring, and band II at ~260 nm, which is the contribution by the A ring [32]. These bands can undergo changes (band shape, position, intensity) as a function of interactions (dispersion, dipole–dipole, H bonding, ionic) established with the solvent [33].

The interaction of rutin with DPBA was studied in some detail by means of spectroscopic titration. In a neutral aqueous solution (phosphate buffer, pH 7), a significant shift of band I to 388 nm on addition of DPBA and the presence of an isosbestic point at 365 nm indicates the formation of a first complex that is in equilibrium with the free flavonoid molecule (Fig. 4b). On further increasing the DPBA concentration, the appearance of a new band at 448 nm suggests the formation of a second adduct. We note that, because all spectra cross at least one of the two isosbestic points, simultaneous presence of free rutin and the two adducts is not feasible, indicating that formation of the second complex starts when all rutin molecules are already involved in the first complex. These data are in accordance with MS data on the presence of two binding sites in the flavonoid molecule which can undergo coordination with DPBA. In order to achieve the stoichiometry of the complexes of rutin with DPBA, we considered the variation in the absorbance at a fixed wavelength as a function of the DPBA-to-flavonoid ratio (Fig. 4c, d). The plot of absorbance at 388 nm versus the molar ratio is indicative of stoichiometry of 1:1 for the first adduct. On the other hand, the second adduct starts to appear beyond a 2:1 molar ratio, and a large amount of DPBA (>100:1) is needed to complete its formation, suggesting a less favoured process.

When the interaction of rutin with DPBA is carried out in absolute ethanol, different dynamics seem to occur at low reagent concentration. In fact, the shift of band I to 411 nm (Fig. 4e, f) via an isosbestic point at 382 nm suggests the formation of a 1:1 complex that is optically different from that previously observed at neutral pH. Moreover, on further increasing the DPBA concentration, the appearance of a shoulder at 450 nm can be ascribed to the incomplete formation of a second adduct with optical characteristics similar to the double complex observed in the aqueous neutral environment.

Sequential appearance of a band peaking at ~410 nm followed by the formation of a shoulder at ~440 nm is apparent during spectroscopic titration of rutin by DPBA under acidic conditions (acetate buffer, pH 4) (Fig. 5a).

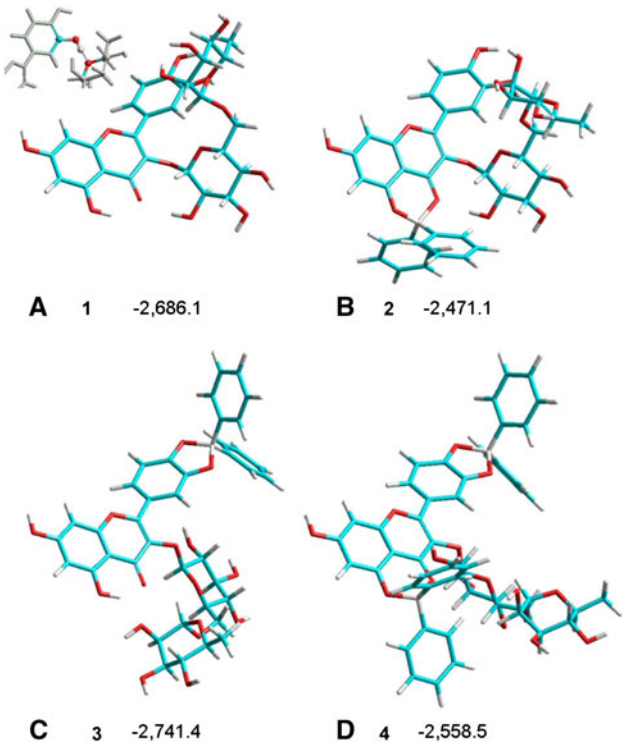

Fig. 6 Representation of the most stable conformation of rutin (**1**, **a**), and complexes **2** (**b**), **3** (**c**), **4** (**d**). Enthalpies of formation are reported in kJ mol^{-1}. The stabilizing H-bond between the O1‴ of the sugar chain and the hydroxyl in 3′ position of the **b** ring of free rutin is magnified in **a**

This finding implies behavior resembling that encountered in ethanol (Fig. 4e). However, the lack of an evident isosbestic point suggests the simultaneous presence of at least three absorbing species in equilibrium. In this case some free rutin molecules were still present even for a large (400:1) excess of DPBA. Overall, the results reveal that the acidic conditions significantly hinder addition of DPBA to both the chelating sites of rutin, resulting in a less favoured complexation process than in neutral buffer and alcohol. These results are in agreement with those from previous studies which highlighted reduced chelating power of flavonols in acidic medium [29] probably ascribed to the presence at low pH of strong intramolecular H-bonds, for example between the 5-hydroxy and the 4-keto group and between the 4′ and 3′ vicinal hydroxyl groups [28], which discourage complexation at these sites.

Table 1 Calculated bond lengths and dihedral angles of rutin (**1**) (from Ref. [26]) and complexes **2**, **3**, and **4**

	1	**2**	**3**	**4**
Bond length/Å				
O1–C2	1.39	1.38	1.39	1.38
O1–C9	1.38	1.38	1.38	1.38
C2–C3	1.37	1.38	1.37	1.39
C3–C4	1.47	1.45	1.46	1.44
C4–C10	1.46	1.42	1.46	1.43
C5–C10	1.42	1.42	1.42	1.42
C5–C6	1.40	1.38	1.40	1.40
C6–C7	1.40	1.41	1.40	1.40
C7–C8	1.40	1.41	1.40	1.41
C8–C9	1.40	1.39	1.40	1.40
C9–C10	1.41	1.41	1.41	1.41
C2–C1′	1.46	1.45	1.46	1.45
C1′–C2′	1.40	1.40	1.41	1.41
C2′–C3′	1.40	1.39	1.39	1.39
C3′–C4′	1.41	1.41	1.44	1.45
C4′–C5′	1.40	1.41	1.39	1.40
C5′–C6′	1.39	1.38	1.40	1.39
C6′–C1′	1.40	1.41	1.40	1.41
C4–O4	1.25	1.29	1.25	1.30
C5–O5	1.36	1.33	1.36	1.34
C7–O7	1.37	1.35	1.37	1.37
C3′–O3′	1.38	1.38	1.36	1.36
C4′–O4′	1.37	1.37	1.34	1.33
Dihedral angle/°				
C2–C3–O3–C1″ = α	131.56	130.02	−121.08	−116.38
C3–O3–C1″–O1″ = ω	−101.26	−97.38	−112.43	−147.16
O1–C2–C1′–C6′ = θ	−36.52	−28.67	−28.74	−22.01
O1″–C5″–C6″–O6″ = γ	84.14	84.94	86.20	74.87
C5″–C6″–O6″–C1‴ = ε	−80.03	175.53	−84.88	−93.35
C6″–O6″–C1‴–O1‴ = δ	−67.46	−69.74	−76.22	−73.81

Under alkaline conditions (sodium acetate, pH 9, Fig. 5b) the spectrum of free rutin is shifted by ~50 nm to longer wavelengths, because of the simultaneous presence of mono and bis-deprotonated forms with deprotonation at the 7 and 4′ positions [34, 35]. In this case, broadening of band I was observed after addition of large (>100-fold) amounts of DPBA, which suggests the generation of DPBA-coordinated anionic species. However, the lack of distinct optical characteristics of the final titration profile prevents more insight being gained into the composition and number of mono or bis adducts at this stage. We note that the large concentration of DPBA required to carry out the complexation process can be ascribed to competition for the boron between the acetate ions of the buffer and the flavonoid anions [30].

The results obtained by spectroscopic analysis make it possible to hypothesize a two-step mechanism of complexation between rutin and DPBA. The first step involves the formation of two possible mono adducts, which are structurally different, depending on the solvent and pH. Neutral and alcoholic conditions are observed to trigger the process whereas the acidic and basic environments seem unfavourable for this step. In the second step, the remaining chelating site of the flavonoid molecule can be involved in a second complexation reaction with DPBA, which necessitates a large excess of the latter, irrespective of the solvent, in order to generate a bis adduct.

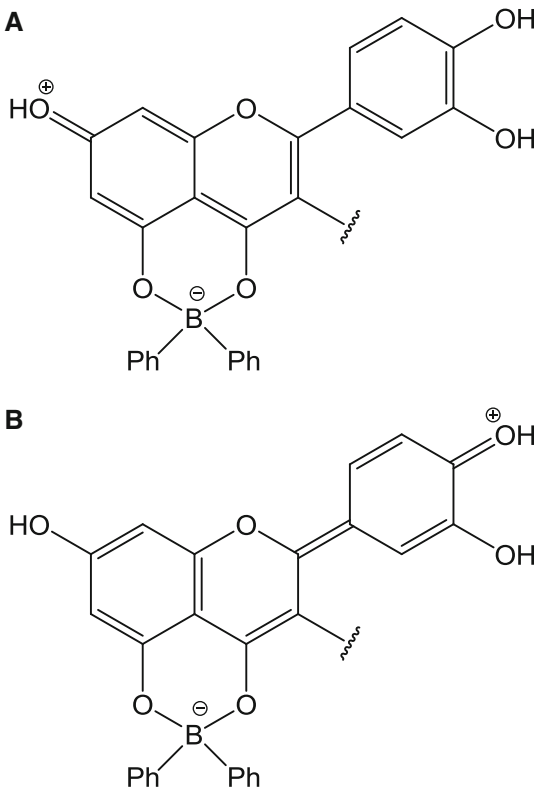

Fig. 7 A-ring (**a**) and B-ring (**b**) quinoid forms of rutin complexed at the ketoenol position

Conformational analysis of complexes

Computational studies were carried out to gain insight into the conformational characteristics of the DPBA–rutin complexes. Different adducts were built by adopting structural data previously found for the most stable conformation of rutin [26] and by using the results from MS. Figure 6 shows the optimized complexed forms after energy minimization with the AM1 semiempirical method, together with their enthalpies of formation.

When DPBA coordinates with the 5-hydroxy-4-keto site (**2**, Fig. 6b), the bond lengths and angles of the A and C rings of rutin are substantially affected (Table 1). The simultaneous decrease in the lengths of the C4–C10, C8–C9, C5–C6, and C7–O7 bonds with an increase in the lengths of the C6–C7 and C7–C8 bonds leads to increased electronic conjugation over the γ-pyrone moiety, which enables us to assume a preponderant weight of an A-ring quinoid form (Fig. 7). Slight shortening of the C3–C4, C2–C1′, C2′–C3′, and C5′–C6′ bonds accompanied by larger C2–C3, C6′–C1′, and C4′–C5′ bonds suggests a minor role of a B-ring quinoid form generated by delocalization of the lone pairs of O4′ over the C ring. The formation of complex **2** leads to a reduction in the angle θ (from approximately $-37°$ to approximately $-29°$), secondary to the breaking of the hydrogen bond between the endocyclic O1‴ of the sugar chain and the hydroxyl in 3′ position of the B ring (Fig. 6a inset). It has previously been noted that this bond stabilizes the free molecule by inducing a folded conformation [26]. The loss of this bond results in reorientation of the rhamnose unit with modification of γ and ε angles.

Coordination of DPBA with the catechol moiety (**3**, Fig. 6c) generates a five-membered ring, which moderately affects all the bonds of the B ring involved in the new complex while leaving the γ-pyrone moiety substantially unaltered. Addition of the DPBA fragment leads to $\sim 110°$ rotation of the α dihedral angle relative to that in free rutin, causing reorientation of the sugar chain and formation of a stable conformation with reduced steric hindrance between the rhamnose unit and the complexed site.

The bis adduct (**4**, Fig. 6d) has features of both complexes **2** and **3**, with reduced participation of an A-ring quinoid form. Compared with the others, formation of this

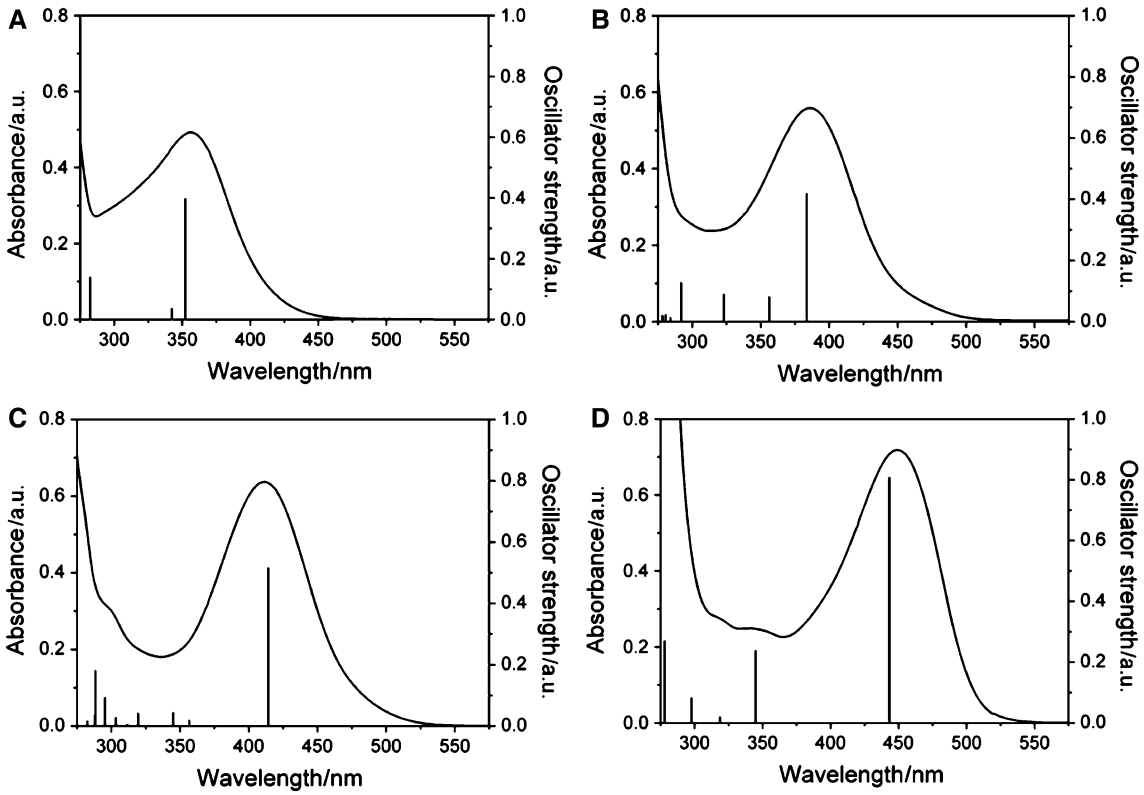

Fig. 8 Comparison of the calculated electronic spectra of uncomplexed rutin (**1**, **a**) and of complexes **2** (**b**), **3** (**c**), and **4** (**d**) with the experimental profiles obtained by spectroscopic titration. The profile obtained from the uncomplexed flavonoid and the profiles of adducts with peaks at 388 and 448 nm (corresponding to 5:1 and 500:1 molar ratios) of Fig. 4b are reported in **a**, **b**, and **d**, respectively. The profile with the peak at 411 nm (corresponding to a 5:1 molar ratio) of Fig. 4e is displayed in **c**. The computational analysis produced profiles which are in excellent agreement with the experimental data. In particular the bathochromic shift of band I on addition of DPBA, which mainly involves the HOMO–LUMO transition [26], is well reproduced by the calculations for the complexed forms

adduct is hindered by simultaneous occupation of the two chelating sites, which compels the rutinoside chain lie on the same plane as the flavonoid moiety in order to minimize the repulsion between the two diphenylboron groups.

Calculated absorption spectra of the most stable conformations of each adduct **2**–**4** were obtained and compared with the experimental spectra (Fig. 8). The results suggest that the chelating site involved in the first complexation step occurring under neutral aqueous conditions can be ascribed to the ketoenol whereas the catechol seems to be the most favoured chelating group in an alcoholic environment and the first to be occupied under acidic conditions.

Rutin is fully protonated in alcoholic solvent and at low pH. In these cases the larger energy stabilization conferred by the addition of a diphenylboron fragment to the catechol moiety rather than the ketoenol site (compare Fig. 6b and c) could be a direct consequence of the preferential generation of complex **3** (although the process is less favored under acidic conditions because of strong intramolecular H-bonding). Conversely, under neutral conditions, the small redshift of band I of free rutin (357 nm, Fig. 4b) compared with that in acidic buffer (350 nm, Fig. 5a), suggests partial involvement of a deprotonated form. In particular, a pK_A of ~ 7 was reported for rutin and ascribed to loss of a proton from one of the most acidic groups, i.e. the 7 [36] or the 4′ [37] hydroxyl groups. We note that deprotonation of 7-OH involves strong electron delocalization toward the γ-pyrone moiety, which thus might favour complexation at the ketoenol site (complex **2**). On the other hand, possible deprotonation at the 4′ position should lead to a minor effect on complexation because of the strong intramolecular H-bond with 3′-OH.

Table 2 Band I position of the absorption spectra of **2a**, **2b**, **3a**, and **4a** calculated by the AM1 semiempirical method

	Band I position/nm
2a	426.5
2b	464.7
3a	376.4
4a	409.1

Conformational analysis of deprotonated complexes

To analyse the spectroscopic profiles obtained by alkaline titration, adducts built by the initial free anionic species were considered. In particular we discuss here the interaction of DPBA with the 7-mono and 7,4′-bis-deprotonated forms of rutin, which, on the basis of previous findings [34, 38], are likely to prevail under the experimental conditions used in this work (buffer at pH 9). The presence of a 4′-monodeprotonated adduct in the final mixture of complexes was regarded as disfavoured, because its energy ($-2{,}560.2$ kJ mol^{-1}) was higher than that of the other anionic complexes; it was therefore excluded from further analysis. Comparison of the experimental (Fig. 5b) and calculated (Table 2) spectroscopic features of the optimized structures suggests the partial formation of a 7-monodeprotonated adduct with the DPBA coordinated to the catechol moiety (**3a**, Fig. 9c) in agreement with a first slight blue-shift of band I, followed by the possible generation of 7-mono and 7,4′-bis-deprotonated species with a complexed 5-hydroxy-4-keto site (**2a** and **2b**, Fig. 9a, b) and of a 7-deprotonated bis adduct (**4a**, Fig. 9d) as implied by the broadening of band I toward higher wavelengths. In this case the initial competition between the ketoenol and catechol sites seems to slightly favour the latter on the basis of energy considerations (compare the enthalpy of complex **3a** with those of complexes **2a** and **2b**).

Structural data for adducts **2a**, **3a**, and **4a** resembled those discussed for **2**, **3**, and **4** with the increased participation of an A-ring quinoid form (Table 3). On the other

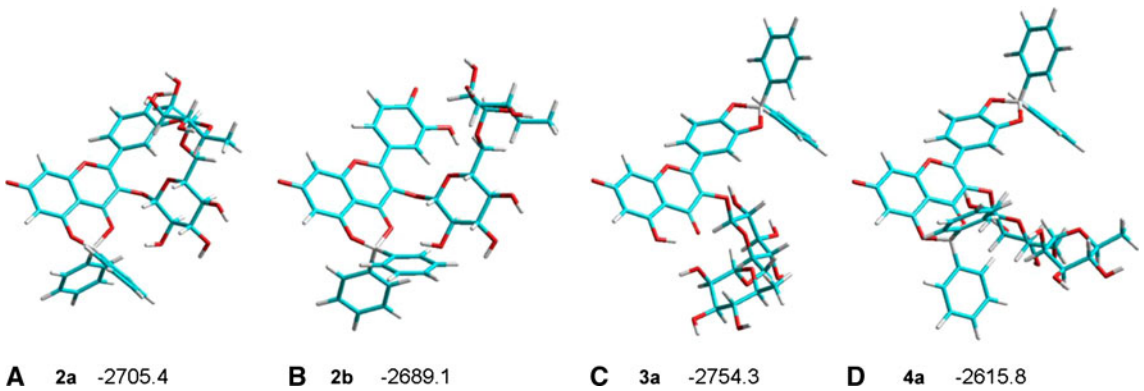

Fig. 9 Representation of the most stable conformation the anionic complexes **2a** (**a**), **2b** (**b**), **3a** (**c**), and **4a** (**d**). Enthalpies of formation are reported in kJ/mol

Table 3 Calculated bond lengths and dihedral angles of complexes **2a**, **2b**, **3a**, and **4a**

	2a	2b	3a	4a
Bond length/Å				
O1–C2	1.38	1.38	1.39	1.38
O1–C9	1.39	1.39	1.39	1.39
C2–C3	1.37	1.40	1.37	1.38
C3–C4	1.46	1.43	1.47	1.45
C4–C10	1.38	1.40	1.44	1.39
C5–C10	1.45	1.43	1.43	1.44
C5–C6	1.37	1.37	1.39	1.37
C6–C7	1.45	1.45	1.45	1.45
C7–C8	1.47	1.46	1.45	1.46
C8–C9	1.36	1.37	1.37	1.36
C9–C10	1.43	1.42	1.42	1.43
C2–C1′	1.47	1.43	1.46	1.46
C1′–C2′	1.40	1.42	1.42	1.42
C2′–C3′	1.39	1.37	1.39	1.38
C3′–C4′	1.41	1.46	1.44	1.44
C4′–C5′	1.41	1.45	1.39	1.39
C5′–C6′	1.39	1.36	1.40	1.40
C6′–C1′	1.41	1.42	1.40	1.40
C4–O4	1.32	1.33	1.25	1.32
C5–O5	1.36	1.36	1.37	1.36
C7–O7	1.25	1.26	1.26	1.25
C3′–O3′	1.38	1.39	1.36	1.36
C4′–O4′	1.37	1.25	1.34	1.35
Dihedral angle/°				
C2–C3–O3–C1″ = α	132.41	122.84	−121.54	−117.92
C3–O3–C1″–O1″ = ω	−104.26	−98.40	−114.50	−149.50
O1–C2–C1′–C6′ = θ	−28.40	−2.69	−30.32	−30.04
O1″–C5″–C6″–O6″ = γ	89.70	106.10	88.04	77.49
C5″–C6″–O6″–C1‴ = ε	175.02	−179.28	−85.82	−91.59
C6″–O6″–C1‴–O1‴ = δ	−71.73	−76.20	−78.86	−77.31

hand, the structural analysis of complex **2b** suggests comparable participation of both A and B-ring quinoid forms, as revealed by the strongly reduced C4′–O4′, C2′–C3′, C5′–C6′, C2–C1′, C3–C4, C4–C10, C5–C6, C8–C9, and C7–O7 bonds associated with the single-bond character assumed by the C3′–C4′, C4′–C5′, C1′–C2′, C6′–C1′, and C2–C3 bonds. In this case, formation of **2b** is supposed to be mainly elicited by delocalization of the negative charges on O7 and O4′ toward the γ-pyrone moiety, which is responsible for a smaller θ angle, leading to a quasi-planar conformation.

Conclusions

In this study, mass spectra, optical spectroscopy measurements, and semiempirical calculations were combined to investigate the chelating mechanism of DPBA with the model flavonoid glycoside rutin. The results suggest that different coordination sites of rutin may be involved, depending on the properties of the medium. Furthermore, whereas pure alcohol and neutral aqueous conditions are found to trigger the chelation process leading to characteristic adducts, in acid or basic aqueous buffers the complexation is less promoted and a mixture of complexed forms is expected. Overall, these findings reveal the possibility of improving existing analytical assays used for flavonoid recognition, by choosing suitable experimental conditions, with the potential to discriminate among different flavonoid moieties. In this context, different responses may be obtained by varying the concentration of added reagent and the pH or type (e.g. alcoholic versus aqueous) of medium adopted.

Experimental

Rutin was purchased from Extrasinthèse (Lyon, Nord-Genay, France). DPBA, phosphate buffer, sodium acetate, and acetic acid (Sigma, St Louis, MO, USA) were used without purification. Flavonoid compounds were dissolved in absolute ethanol (Merck, Darmstadt, Germany) at a concentration of 1×10^{-3} mol dm^{-3} and kept in the dark at − 18 °C until the measurements were performed.

Mass spectra were acquired with a HP-1100 liquid chromatograph equipped with a DAD detector and a HP 1100 MSD API-electrospray (Agilent Technologies, Palo Alto, USA) operating in negative-ionization mode, as reported previously [39]. Detailed conditions were: gas temperature 350 °C, capillary potential 3,500–4,000 V, nebulizer pressure 30 psi, quadrupole temperature 30 °C, and capillary potential 3,500 V. The fragmentor operated at 80 eV. The experiments were conducted on 40×10^{-6} mol dm^{-3} solutions in pure water obtained by diluting standard stock solutions. A 1 to 5% (*w*/*v*) ethanolic solution of DPBA was added to rutin in order to obtain a final 1:1 to 100:1 [DPBA]/[rutin] ratio. A 80:20 mixture of water–CH_3CN was used as eluent for FIA (flow injection analysis) and HPLC analysis of rutin samples.

The UV–visible absorption spectra of rutin solutions before and after addition of DPBA were recorded by use of a Jasco (Tokyo, Japan) 560 V UV–visible spectrophotometer with 1-cm path-length sample cells. Rutin samples (40×10^{-6} mol dm^{-3}) were obtained by diluting stock solutions with ethanol, phosphate buffer (0.1 mol dm^{-3}, pH 7), acetate buffer (0.1 mol dm^{-3}, pH 4), or sodium acetate (0.1 mol dm^{-3}, pH 9). Spectroscopic titrations were conducted by following the molar ratio method, which furnishes the composition of the complexes from spectrophotometric data [35]. In this method, the

concentration of rutin was kept constant whereas the DPBA concentration was varied from 1 to 500-fold the molar concentration of the flavonoid.

The semiempirical method Austin Model 1 (AM1) was adopted to find the most stable conformations of the adducts between rutin and DPBA, in accordance with previous work [26]. Energy minimization was performed by use of the Polak–Ribière algorithm with a convergence criterion of 0.004 kJ mol^{-1}. The electronic absorption spectra of the most stable conformers were calculated by use of a configuration interaction (CI) treatment. This calculation accounted for the contribution of singly excited configurations involving the nine highest occupied and the nine lowest unoccupied molecular orbitals. The calculations were performed by use of Hyperchem (version 7.5) software on a Pentium 4 3.20-GHz computer.

References

1. Harborne JB, Williams CA (2000) Phytochemistry 55:481
2. Pfündel EE, Agati G, Cerovic ZG (2006) Optical properties of plant surfaces. In: Riederer M, Müller C (eds) Biology of the Plant Cuticle. Annu Plant Rev, vol 23. Blackwell, Oxford, p 215
3. Pietta PG (2000) J Nat Prod 63:1035
4. Agati G, Tattini M (2010) New Phytol 186:786
5. Jordan BR (2002) Funct Plant Biol 29:909
6. Choquenet B, Couteau C, Paparis E, Coiffard L (2008) J Nat Prod 71:1117
7. Reuber S, Bornman JF, Weissenböck G (1996) Physiol Plant 97:160
8. Agati G, Matteini P, Goti A, Tattini M (2007) New Phytol 174:77
9. Schoch G, Goepfert S, Morant M, Hehn A, Meyer D, Ullmann P, Werck-Reichhart D (2001) J Biol Chem 276:36566
10. Hernández I, Alegre L, Van Breusegem F, Munné-Bosch S (2009) Trends Plant Sci 14:125
11. Rice-Evans CA, Miller NJ, Paganga G (1997) Trends Plant Sci 2:152
12. Sichel G, Corsaro C, Scalia M, Di Bilio AJ, Bonomo RP (1991) Free Radic Biol Med 11:1
13. Hutzler P, Fischbach R, Heller W, Jungblut TP, Reuber S, Schmitz R, Veit M, Weissenbock G, Schnitzler JP (1998) J Exp Bot 49:953
14. Gould KS, McKelvie J, Markham KR (2002) Plant Cell Environ 2002:1261
15. Peer WA, Brown DE, Tague BW, Muday GK, Taiz L, Murphy AS (2001) Plant Physiol 126:536
16. Homberg H, Geiger H (1980) Phytochemistry 19:2443
17. Kartnig T, Göbel I (1996) J Chromatogr A 740:99
18. Neu R (1957) Naturwissenschaften 44:181
19. Schnitzler JP, Jungblut TP, Heller W, Kofferlein M, Hutzler P, Heinzmann U, Schmelzer E, Ernst D, Langebartels C, Sandermann H (1996) New Phytol 132:247
20. Tattini M, Galardi C, Pinelli P, Massai R, Remorini D, Agati G (2004) New Phytol 163:547
21. Sheahan JJ, Cheong H, Rechnitz GA (1998) Am J Bot 85:467
22. Valette C, Andary C, Geiger JP, Sarah JL, Nicole M (1998) Phytopathology 88:1141
23. De la Rosa L, Alvarez-Parrilla E, Gonzalez-Aguilar GA (2010) Fruits and vegetable phytochemicals. Wiley-Blackwell, Singapore
24. Ren W, Qiao Z, Wang H, Zhu L, Zhang L (2003) Med Res Rev 23:519
25. Wang HK (2000) Expert Opin Investig Drugs 9:2103
26. Matteini P, Goti A, Agati G (2010) Monatsh Chem 141:793
27. Roshal AD, Munos O, Sakhno TV, Buadon MT (2002) Chem Heterocycl Compd 38:1412
28. Cornard JP, Boudet AC, Merlin JC (2001) Spectrochim Acta A Mol Biomol Spectrosc 57:591
29. Cornard JP, Merlin JC (2002) J Inorg Biochem 92:19
30. Cornard JP, Merlin JC (2001) J Mol Struct 569:129
31. Yan Y, Springsteen G, Deeter S, Wang B (2004) Tetrahedron 60:11205
32. Mabry TJ, Markham KR, Thomas MB (1970) The systematic identification of flavonoids. Springer, Berlin
33. Zsila F, Bikádi Z, Simonyi M (2003) Biochem Pharmacol 65:447
34. Escandar GM, Sala LF (1991) Can J Chem 69:1994
35. Cornard JP, Merlin JC (2002) Polyhedron 21:2801
36. Jurd L, Horowitz RM (1957) J Org Chem 22:1618
37. Sauerwald N, Schwenk M, Polster J, Bengsch E (1998) Z Naturforsch B 15:315
38. Lemanska K, Szymusiak H, Tyrakowska B, Zielinski R, Soffers AE, Rietjens IM (2001) Free Radic Biol Med 31:869
39. Saracini E, Tattini M, Traversi ML, Vincieri FF, Pinelli P (2005) Chromatographia 62:245